EFDA–JET–CP(14)03/12

P. Mantica, C. Angioni, F.J. Casson, T. Pütterich, M. Valisa,
M. Baruzzo, P.C. da Silva Ares-ta Belo, I. Coffey, P. Drewelow,
C. Giroud, N.C. Hawkes, T.C. Hender, T. Koskela, L. Lauro Taroni,
E. Lerche, C.F. Maggi, J.Mlynar, M. O'Mullane, M.E. Puiatti,
M.L. Reinke, M. Romanelli and JET EFDA contributors

Understanding and Controlling Tungsten Accumulation in JET Plasmas with the ITER-like Wall

Understanding and Controlling Tungsten Accumulation in JET Plasmas with the ITER-like Wall

P. Mantica[1], C. Angioni[2], F.J. Casson[3], T. Pütterich[2], M. Valisa[4], M. Baruzzo[4], P.C. da Silva Ares-ta Belo[5], I. Coffey[3], P. Drewelow[2], C. Giroud[3], N.C. Hawkes[3], T.C. Hender[3], T. Koskela[6], L. Lauro Taroni[4], E. Lerche[7], C.F. Maggi[2], J.Mlynar[8], M. O'Mullane[3], M.E. Puiatti[4], M.L. Reinke[9], M. Romanelli[3] and JET EFDA contributors*

JET-EFDA, Culham Science Centre, OX14 3DB, Abingdon, UK

[1]Istituto di Fisica del Plasma, CNR/ENEA, Milano, Italy
[2]Max Planck Institut fur Plasmaphysik, Garching, Germany
[3]CCFE, Culham Science Centre, Abingdon, OX14 3DB, UK
[4]Consorzio RFX– CNR/ENEA, Padova, Italy
[5]Instituto de Plasmas e Fusao Nuclear, IST, Lisbon, Portugal
[6]Aalto University, Tekes, P.O.Box 14100, FIN-00076 Aalto, Finland
[7]LPP-ERM-KMS, Belgian State, TEC partner, Brussels, Belgium
[8]IPP.CR, Institute of Plasma Physics AS CR, Prague, Czech Republic
[9]York Plasma Institute, Department of Physics, University of York, Heslington, York YO10 5DD, UK
** See annex of F. Romanelli et al, "Overview of JET Results", (24th IAEA Fusion Energy Conference, San Diego, USA (2012)).*

Preprint of Paper to be submitted for publication in Proceedings of the
41st EPS Conference on Plasma Physics, Berlin, Germany
23rd June 2014 – 27th June 2014

INTRODUCTION

The development of H-mode scenarios in JET with ITER-like wall (ILW) has indicated the need of understanding and controlling W accumulation, which hinders the attainment of good confinement for long durations [1,2]. This paper presents experimental results, interpretative modeling and theory predictions of W transport in JET ILW standard H-mode (STH) and Hybrid plasmas, including first results of heavy impurity Laser Blow-offs (LBO). A key element for the understanding has been the availability of theory models for W neoclassical and turbulent transport (NEO [3] and GKW [4] respectively) that include the effects of rotation on transport coefficients and poloidal asymmetries.

The typical pattern towards W accumulation has been identified in a Hybrid discharge [2] as due to progressive peaking of the density [5] and reversal of neoclassical convection from outward to inward, but is in fact common to both scenarios, as can be seen from the time traces shown in Figure 1. Both discharges feature NBI heating only and show similar time evolution of the density profiles and SXR emission (Figure 1 d and e). In the STH however the more regular and frequent sawtooth activity (Figure 2) limits the central W peaking, allowing attainment of a stationary discharge, which in Hybrids is not possible (Figure 1b). The sawtooth activity seems a better candidate than ELMs to explain the difference in stationarity in STHs vs Hybrids, because ELMs, although more frequent in STH (Figure 2), regulate the W influx from the edge rather than its spatial profile. So the presence of regular ELMs is a necessary condition in both scenarios to reduce the W influx and avoid high W contamination, but it is only a central expulsion mechanism like MHD crashes that can counteract the unfavourable transport that causes central accumulation.

Referring to [2] for the detailed analysis and NEO+GKW simulations of the Hybrid shot, in this paper we present the analogous study for the STH discharge. The 3 times at which the simulations have been performed are 9.34s, 10.42s and 12.37s, taken at the top of sawteeth in 3 different phases of the discharge. The density profiles and the SXR tomographic reconstructions for these 3 times are shown in Figures 3 and 4. One can see the hollow initial n_e profile leading to hollow W density (peaking at the LFS due to centrifugal effects), and the progressive n_e peaking leading to centrally peaked W profile, with intermediate phases in which both the LFS and central peaks coexist (t = 10.42s).

In Figure 6 the W density (n_W) profiles in the equatorial plane obtained by the NEO+GKW simulations made with the same procedure described in [2] at the 3 chosen times are compared with the n_W profiles reconstructed experimentally from the 2D SXR emission using the analyzer also described in detail in [2]. The NEO+GKW W V/D profiles are shown in Figure 5, where one can see the reversal of the neoclassical convection when n_e peaks. The agreement between theory and experiment is good taking into account the experimental uncertainties. In particular we note that at t = 9.34 s the experimental SXR analysis possibly due to the constraint of constant Zeff yields a rotation slightly smaller than measured by the CX diagnostic, and this is responsible for the larger hump at HFS with respect to the NEO+GKW simulation which uses the measured CX rotation. These results constitute a further validation of the NEO+GKW W transport theory against JET

data. It is important to note that for this discharge the inclusion of centrifugal effects is crucial not only for the poloidal mapping but also for the transport calculations. In fact Figure 6 also shows (dashed line) the n_W profiles calculated including centrifugal effects in poloidal mapping but not in transport, indicating that both are indeed required to match the data.

Having understood that all high power JET NBI plasmas are prone to W accumulation due to density peaking, to which the unavoidable core NBI particle source is a main contributor as discussed in [6], the only possible path to controlling accumulation relies in application of strong ICRH on-axis heating. Indeed, first attempts in standard H-mode plasmas with 6 MW ICRH have been successful in preventing W accumulation [7]. ICRH has various effects that all contribute to suppressing W accumulation. First, it affects main plasma profiles, typically causing n_e flattening and T_i peaking, thereby reducing the neoclassical inward convection. Second, the minority fast ion temperature also contributes to neoclassical screening. Third, the anisotropy of the fast ion temperature reduces the W diffusion, enhancing the effects of convection. These effects are analyzed in detail through NEO+GKW simulations in [8]. In the following we present initial experimental results of laser blow-offs (LBO) in STH plasmas without and with ICRH. Both W and Mo were injected, but Mo turned out to be the best diagnosed via the SXR cameras, since their filters cut off most of the W line emission. Figure 7 shows plasma profiles just before the Mo injections for 85308 (19.1MW NBI) and 85307 (14.7MW NBI+ 4.9MW ICRH in (H)-D). We note the n_e flattening due to ICRH, which reduces the inward convection, whilst T_i is not changed. Figure 9 compares for the two cases with and without ICRH, the experimental SXR line integrals at one representative position, together with time dependent 1.5D JETTO-SANCO [9] simulations in which empirical profiles of Mo diffusion and convection are adjusted iteratively in order to best fit the experiment, calculating the SXR line integrals with the UTC SXR post-processor. Figure 8 shows the Mo D and v profiles obtained by such optimization procedure. Figure 10 shows for the discharge without ICRH the spatial profile of the SXR line integrated emission from a vertical camera together with the JETTO-SANCO simulation, 140 ms after the LBO. While in the discharge with ICRH the background plasma is almost stationary during the LBO phase, in the discharge without RF injection the dynamics of W through the sawtooth period, which produces the central emission peak in Figure 10, must be considered. These experimental results indicate beyond the experimental uncertainties that the main change in heavy impurity transport due to ICRH is the reversal of the sign of neoclassical convection. In [8] it is found that ICRH fast ion effects are important in addition to n_e flattening to explain this experimental evidence. Increase of central turbulent diffusivity, often invoked to explain W control by central RF heating [10], does not seem to play an important role in these JET experiments.

This work was supported by EURATOM and carried out within the framework of EFDA. The views and opinions expressed herein do not necessarily reflect those of the European Commission.

REFERENCES

[1]. F. Romanelli, Nuclear Fusion **53** (2013) 104002

[2]. C. Angioni et al., accepted by Nuclear Fusion

[3]. E. Belli and J. Candy, Plasma Physics and Controlled Fusion **54** (2012) 015015

[4]. F.J. Casson et al., Physics of Plasmas **17** (2010) 102305

[5]. A. Loarte et al., Nuclear Fusion **53** (2013) 083031

[6]. P. Mantica et al., Proc. 40th EPS Conference on Plasma Physics, Espoo, 2013, ECA Vol.37D, P4–141 (2013)

[7]. D. Van Eester et al., this conference

[8]. F.J. Casson et al., invited talk at this conference

[9]. L. Lauro Taroni et al., Proc. 21st EPS Conference Controlled Fusion and Plasma Physics, Montpellier, France, **Vol. I**, p. 102 (1994)

[10]. R. Dux et al., Plasma Physics and Controlled Fusion **45**, (2003) 1815

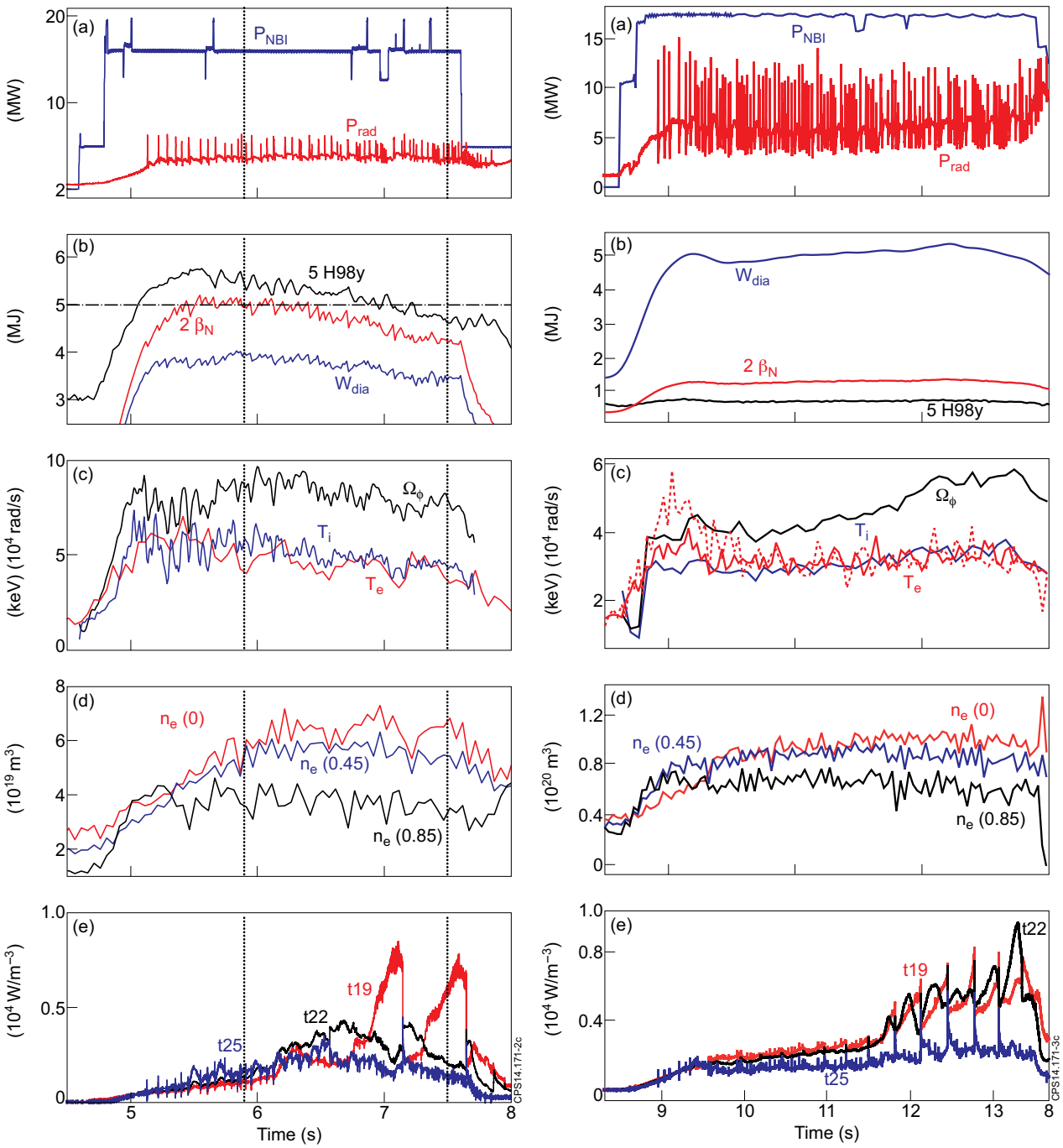

Figure 1: Main time traces of discharge 82722 on the left (Hybrid, B_T = 2 T, Ip = 1.7 MA) and 83351 on the right (standard H-mode, B_T = 2.6 T, Ip = 2.75 MA). t19, t22 and t25 are SXR line integrals with tangency radius respectively at r/a = 0, 0.22, 0.4. The dashed lines indicate the times for the NEO+GKW modeling.

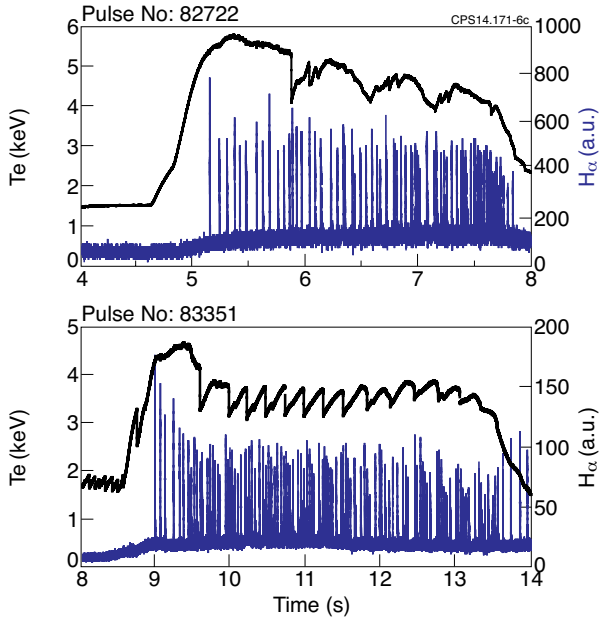

Figure 2: Central Te and H-α emission for discharges 82722 (Hybrid) and 83351 (STH).

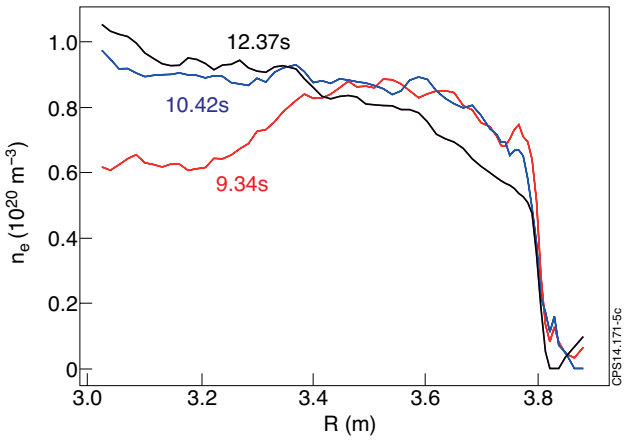

Figure 3: n_e profiles for shot 83351 at the 3 times chosen for NEO+GKW simulations.

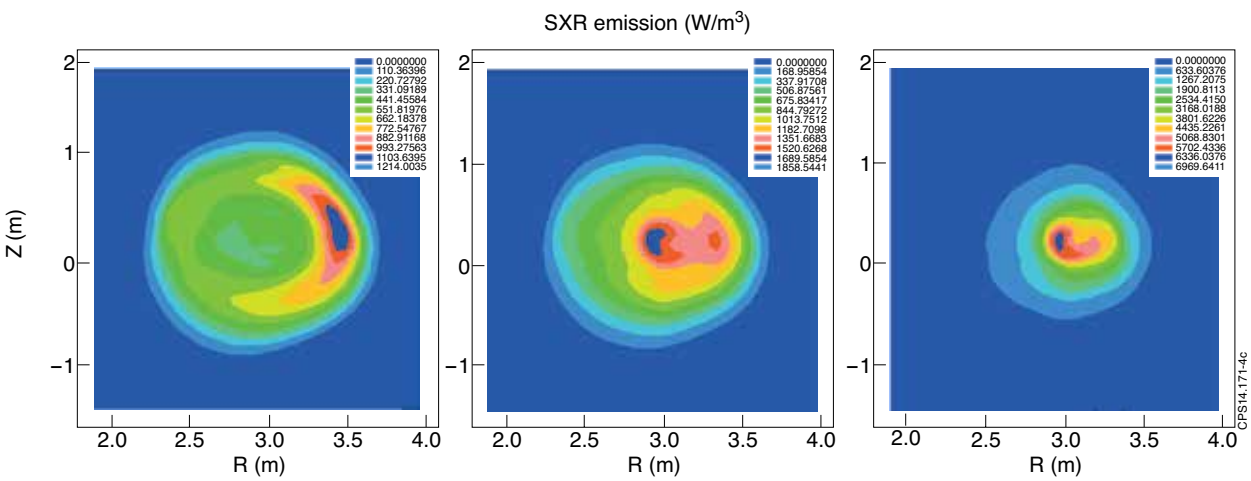

Figure 4: tomographic reconstruction of SXR emission for shot 83351 at the 3 times chosen for NEO+GKW simulations.

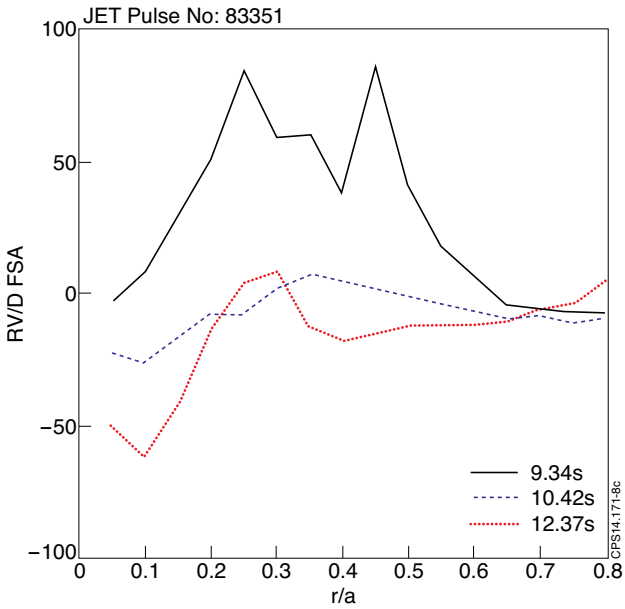

Figure 5: W D/v profiles averaged over the flux surface calculated by NEO+ GKW for shot 83351 at the 3 chosen times.

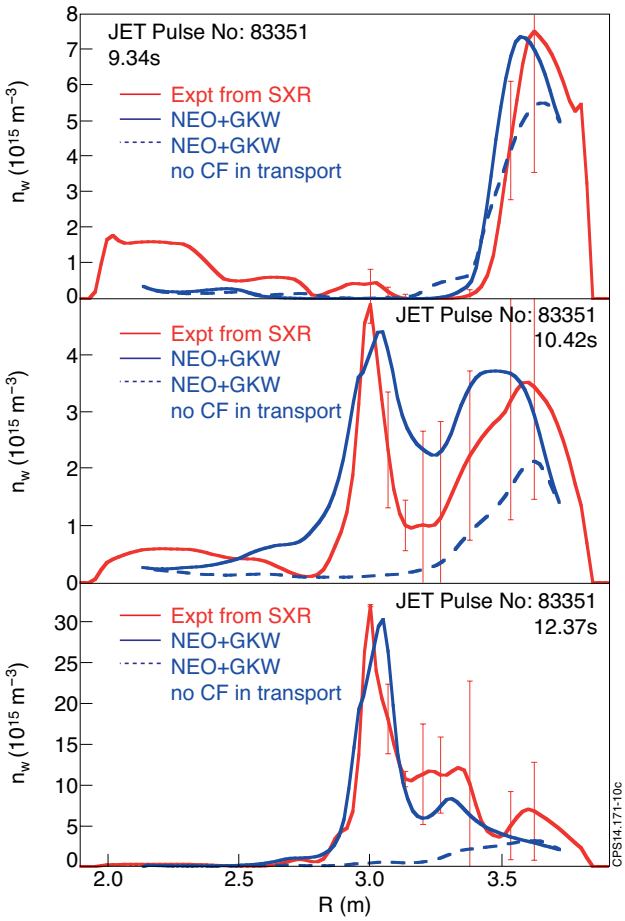

Figure 6: W density profiles calculated by NEO+GKW for shot 83351 at the 3 chosen times, compared with those deduced from the SXR emission measurements. The dashed line is the result of simulations where centrifugal effects are not included in the transport calculation but only in the poloidal mapping.

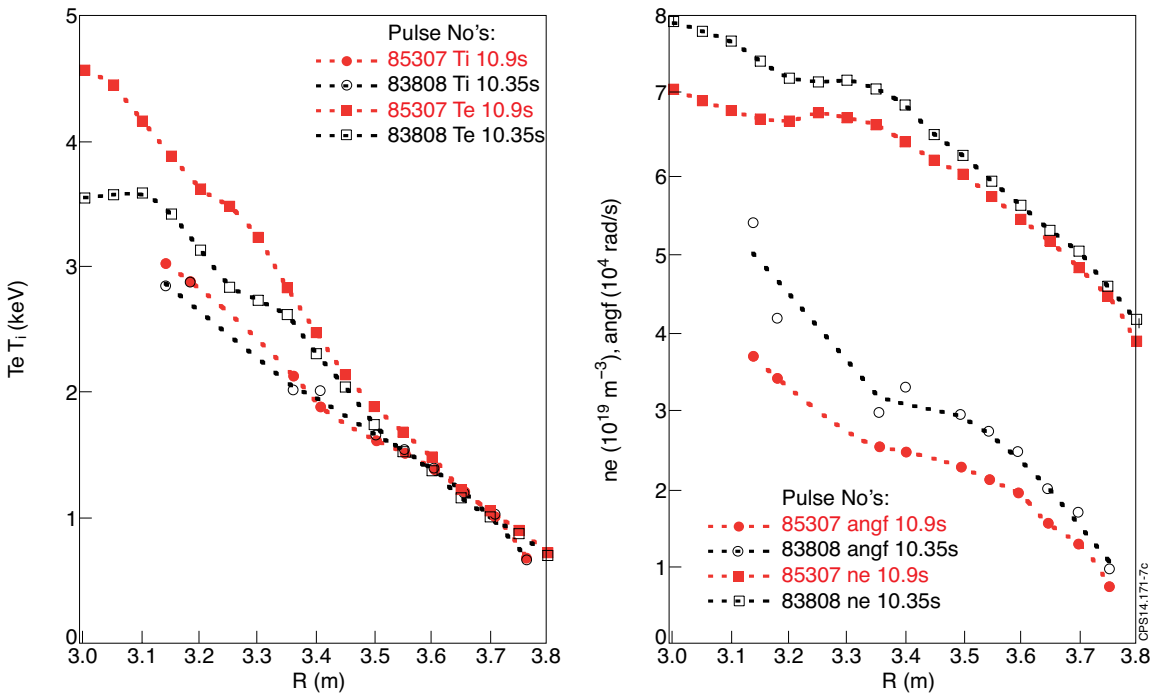

Figure 7: T_i, T_e, n_e and rotation profiles just before LBO in STH discharges with NBI only (85308, black) and with ICRH (85307, red).

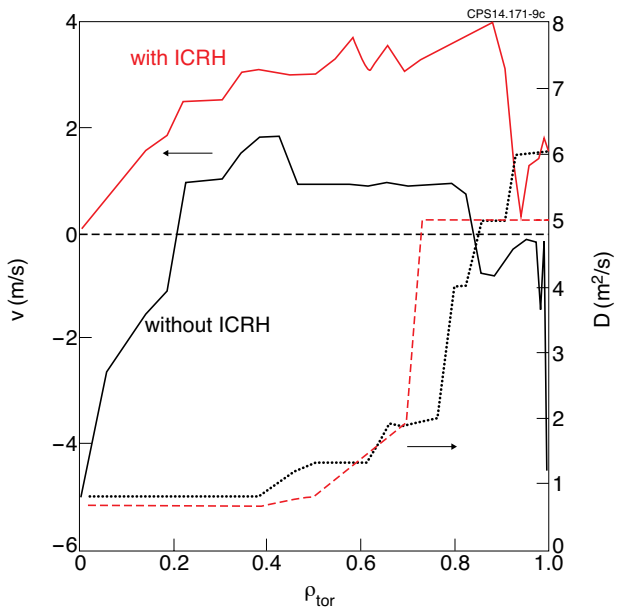

Figure 8: Mo D (dashed) and v (full) FSA profiles from time dependent simulations using JETTO-SANCO of MO blow-off in STH discharges without (black, 85308) and with (red, 85307) ICRH.

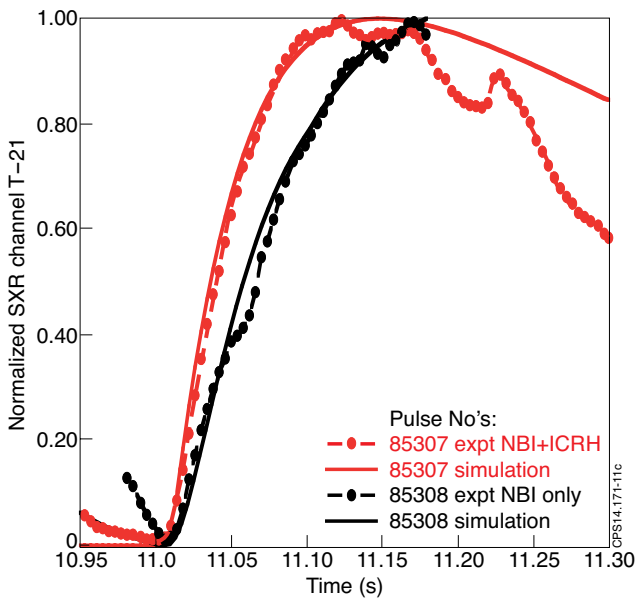

Figure 9: SXR Channel #21 of the vertical camera T (dashed line) and JETTO-SANCO simulations for Mo LBO in shot 85308 (black, NBI only) and shot 85307 (red, NBI+ ICRH). The growth of the SXR trace after the LBO is much slower in the NBI-only case.

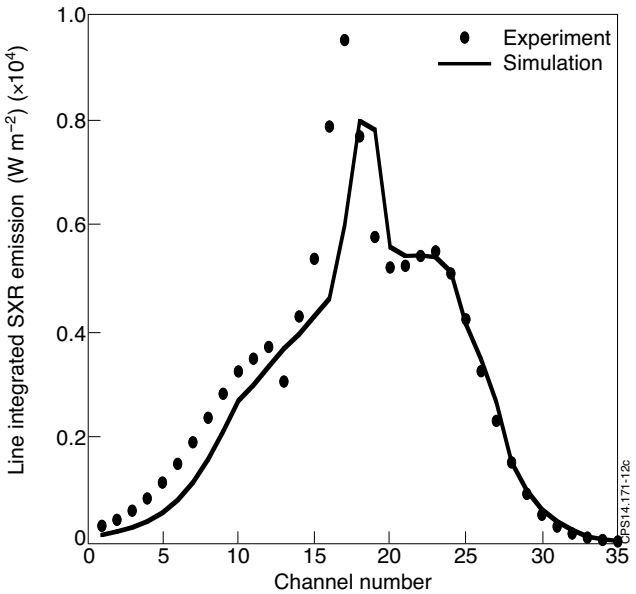

Figure 10. Profile of the vertical SXR camera T 0.14 sec after the LBO of Mo into the 85308 NBI only discharge. Green triangles are the expt data and blue stars are the JETTO-SANCO simulations. The Mo signature is represented by the bulge on the right, while the central peak is due to W.